Further Development of Mathematical Models for Free Burning Electric Arcs

Boyan E. Djakov, Leonid M. Shpanin *Senior Member, IEEE*, Gordon R. Jones, Joseph W. Spencer and Jiu Dun Yan, *Senior Member, IEEE*

***Abstract*—A mathematical model predicting the electric arc plasma behavior in air, atmospheric pressure is developed. Modeling algorithms are reported for free burning (rather than wall stabilized) dc-arc parameters, such as: the arc radial temperature distribution T(r), electric field E along the arc column, arc radius r_0 (radius of the electrically conductive zone $\sigma > 0$). Such arcs may have more complex structures than wall stabilized arcs. Examples of such arcs are electromagnetically rotated arcs, electric arc furnaces, lightning return stroke (LRS). By comparison with experimental data and with more precise calculations the model was validated practically and theoretically and form the basis for investigating the behaviour of complex electromagnetically convoluted arcs in the process of interrupting Direct Currents.**

***Index Terms*—Arc modeling, arc discharges, arc plasma devices, plasma control, current interruption.**

I. Introduction

Theoretical studies of high current electric arcs have been based on Elenbaas-Heller equations (e.g. Steenbeck, Maecker) [1-5]. Subsequent calculations of arc properties have been based upon several (at least 6) forms of analytical/numerical theoretical models [2]. The arcs considered have been limited to cylindrical arcs (wall stabilized) in atomic gases or nitrogen. The present contribution is concerned with addressing various types of free burning (self-stabilized) arcs in air which are of a more complex nature (e.g. Figure 1a, b, c). The approach is based upon approximation made by Zarudi (quasi-channel model) [1] since it provides a compromise between simplicity and accuracy.

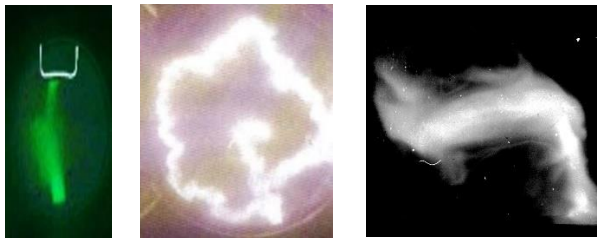

(a) (b) (c)

Fig. 1. Examples of arcs of different forms. a) Axisymmetric arc in linear gas flow; b) Inner and c) Outer magnetic field driven rotating arcs [7].

Manuscript received July 15th, 2023;
(Corresponding author: B. E. Djakov).

Boyan E. Djakov, is with the NUCLEUS Plasma Test Laboratory, building of the Institute of Electronics, Bulgarian Academy of Sciences, BG-1784 Sofia, Bulgaria (e-mail: boyan@djakov.com).

Leonid M. Shpanin, is with the Department of Engineering and Mathematics, Sheffield Hallam University, S1 1WB, Sheffield, UK (e-mail: L.Shpanin@shu.ac.uk).

For example, 2D and 3D arc models are computationally expensive [6-7] as they require the numerical solution of the governing equation(s) based on a grid system. The present approach is 1D [1] and it provides information about the arc characteristics to an acceptable accuracy yet in a rapid manner.

Zarudi's approach has been shown for argon to provide reasonably precise results compared with three different versions of Maecker's approach plus results of reference numerical simulations [1].

The present contribution addresses the following:

- numerical values for the molecular transport coefficients (experimentally measured and/or theoretically predicted) are selected for air at atmospheric pressure and temperature in the range of 4000K to 22000K;
- mathematical expressions and numerical values are produced to represent the changes in the properties;
- a description of physical features and mathematical formalism of the model is made;
- calculations are made for the above range of temperatures;

Numerical results obtained from the calculations are compared with experimental measurements and with a solution of the exact Elenbaas-Heller equations. The approach provides a means for addressing economically the behaviour of a wide range of arcing conditions which exist in various practical devices (e.g. convoluted arcs in electromagnetically controlled circuit breakers (Figure 1b), [6-8], arc furnaces [9, 10] etc.). In principle, the model can be used for higher pressures.

II. Transport Properties of Air at High Temperatures

Thermal & Electrical Conductivity and Optical Emissivity

The Elenbaas-Heller's theoretical description of the electric arc column requires detailed knowledge of three physical mechanisms (microscopical i.e., at the atomic level):

1) Production of thermal energy by Joule heating.
2) Dissipation of the thermal energy by conduction of heat and optical radiation.
3) Transport of electric charge (electric current flow).

Gordon R. Jones, Joseph W. Spencer, Joseph Yan are with the Department of Electrical Engineering and Electronics, University of Liverpool, L69 3GJ, UK (e-mail: grjones@liverpool.ac.uk; joe@liverpool.ac.uk; yaneee@liverpool.ac.uk).

For several atomic and molecular gases, including dry air, the thermal and electrical conductivities as well as optical radiation characteristics at high temperatures have been widely studied both experimentally and theoretically [1-5, 11].

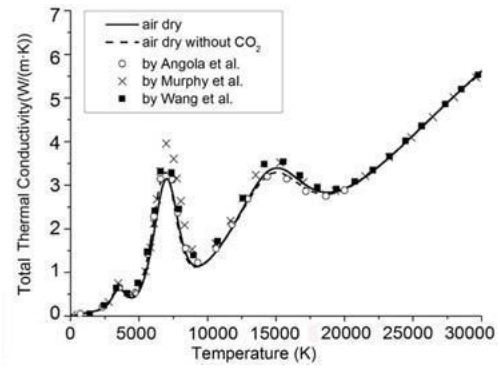

(a)

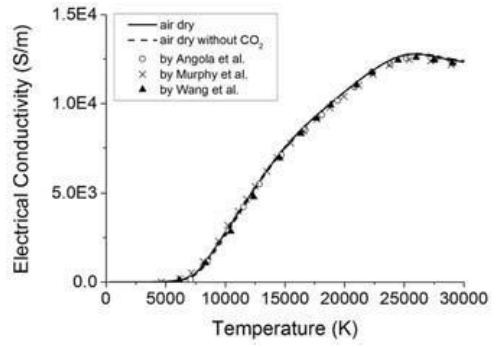

(b)

Fig. 2. Variation of dry air properties at atmospheric pressure with temperature (a) Thermal conductivity, (b) Electrical conductivity (Wang *et al* [12]).

Most of the publications deal with plasma in thermal equilibrium. Calculated and measured data by various authors may differ by 10 to 25% for transport coefficients and by about 50% for optical properties [1, 2, 12, 13].

TABLE I

OPTICAL EMISSIVITY ε OF FLAT AND HEMISPHERICAL AIR SAMPLES AS A FUNCTION OF TEMPERATURE ALONG WITH THE MEAN OF BOTH PARAMETERS, (Avilova *et al* [13]).

T, (K)	$\dot{\varepsilon}$ (flat)	$\dot{\varepsilon}$ (hemispherical)	ε = [$\dot{\varepsilon}$ (flat) + $\dot{\varepsilon}$ (hemispherical)]/2
8000	4.0×10^{-4}	2.3×10^{-4}	3.15×10^{-4}
9000	8.8×10^{-4}	5.6×10^{-4}	7.2×10^{-4}
10000	2.3×10^{-3}	1.5×10^{-3}	1.9×10^{-3}
11000	5.0×10^{-3}	3.5×10^{-3}	4.25×10^{-3}
12000	9.6×10^{-3}	6.7×10^{-3}	8.15×10^{-3}
13000	1.6×10^{-2}	1.1×10^{-2}	1.35×10^{-2}
14000	2.1×10^{-2}	1.5×10^{-2}	1.8×10^{-2}
16000	2.6×10^{-2}	1.8×10^{-2}	2.2×10^{-2}
18000	2.2×10^{-2}	1.4×10^{-2}	1.8×10^{-2}
20000	1.6×10^{-2}	8.7×10^{-3}	1.24×10^{-2}

For dry air at atmospheric pressure, the variation of thermal (λ) and electrical (σ) conductivities from Wang *et al* [12] are shown in Figures 2a and Figure 2b.

For the optical radiation the power flux density is given by

$$q(T) = \varepsilon(T)\,\kappa\,T^4 \tag{1}$$

where: $\kappa = 5.67\times10^{-8}$ W/(m^{2}K^4) is the Stefan-Boltzmann constant and ε (T) is the dimensionless optical emissivity. The optical emissivity ε from tabulated numerical data (Table I) by Avilova *et al* [13] for emitting plasma samples of two shapes, flat, $\dot{\varepsilon}$ (flat) and hemispherical, $\dot{\varepsilon}$ (hemispherical), all these parameter values are as a function of the gas temperature T assuming an LTE state for the gas.

Data processing is performed in several stages *1*, *2* and *3*:

1. Conversion of Data from Graphical to Numerical Form

The read-out from the intersecting points with the axes of the graphs provides numerical values of λ and σ that correspond to temperatures from the minimal (where σ = 0 is assumed) to 22000K in steps of 500K, in some cases of 1000K. In the present work, it can be shown that the peaks in material property data set are resolved using the selected interval. Thus, a large discrepancy in results is not expected.

Tabulated data for the emissivity ε are selected for T ≥ 7000K, atmospheric pressure and thickness of the emitting layer of 1cm. For atmospheric pressure and 1 cm thick layer [13] within the important temperature range (>14000K) emissivity ε is changed by about 35% for 50% change of optical thickness. The dependencies λ(T), σ(T), and ε(T) are then available in the form of tables. For ε(T) two sets of numbers are obtained - one for a flat emitting layer and another for a hemispherical layer (Table I). The model being developed here deals with cylindrical plasma columns which radiate at a rate somewhere in between the two cases, where the thickness is equal to the radius, and it is a matter of geometry and independent of conditions. It is assumed that in this case the power of emission is an average of these two values ε = [$\dot{\varepsilon}$ (flat) + $\dot{\varepsilon}$ (hemispherical)]/2, (Table I).

2. Conversion of Data from Numerical to Analytical Form

Conversion of data from numerical to analytical form is achieved by approximation with elementary functions [14] and the use of TableCurve2D software [15], (TC2D).

a) The thermal conductivity λ (T) as a function of temperature (T) is given by

$$\lambda(T) = \sum_{i=0}^{N} \alpha_i\,(T/1000)^i \tag{2}$$

where: α_i and N are parameters determined from the relationship between λ (T) in [W/ (m K)] and temperature (T) in [K] (Figure 2a). For the present case N = 7, α_0= -272, α_1 = 159, α_2 = -36.7, α_3 = 4.43, α_4 = -0.304, α_5 = 0.0119, $\alpha_6 = -2.50\times10^{-4}$, $\alpha_7 = 2.17\times10^{-6}$ are polynomial coefficients, and r^2 = 0.9943 is the correlation factor [15]. Using the TC2D software [15], the polynomial fit of the equation (1) is based on 16 points for the temperature range 7000K ≤ T ≤ 22000K and is created and shown in Figure 3a. Among different possibilities offered by this software the polynomial fits have the advantage of easy integration in analytical form.

b) The electrical conductivity σ (T) versus temperature is approximated in two temperature ranges 7000K ≤ T ≤ 22000K and 4000K ≤ T ≤ 8000K. For the temperature range 7000K ≤ T ≤ 22000K the electrical conductivity σ (T) relation is,

$$\sigma\,(T) = (\beta_1 + \beta_2/T)^2 \qquad (3a)$$

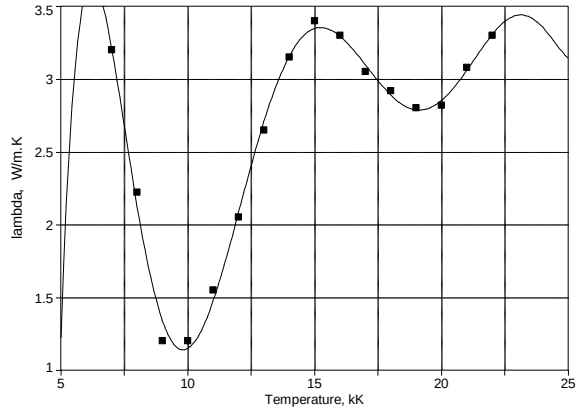

(a) TC2D fit of equation (2) for the thermal conductivity versus temperature, 7000K ≤ T ≤ 22000K

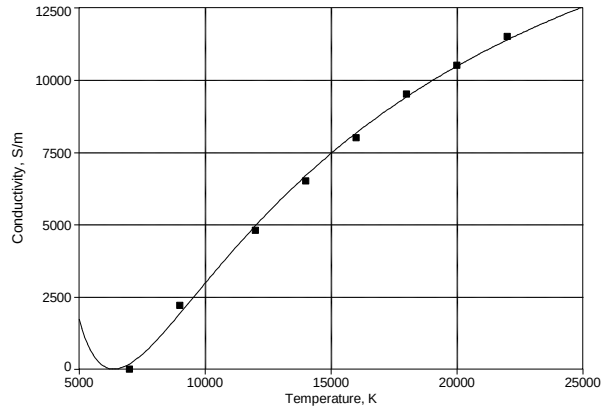

(b) TC2D fit of equation (3a) for the electrical conductivity versus temperature, 7000K ≤ T ≤ 22000K

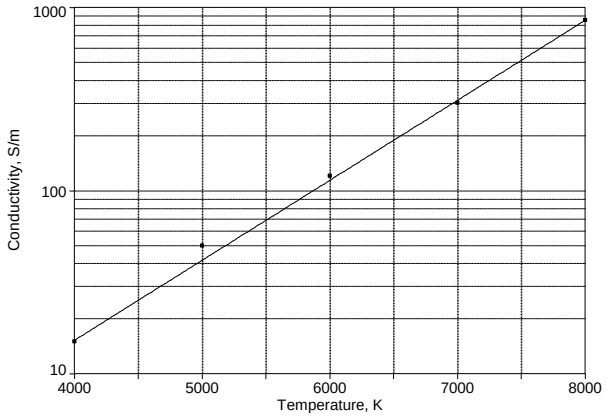

(c) TC2D fit of equation (3b) for the electrical conductivity versus temperature, 4000K ≤ T ≤ 8000K

Fig. 3. TC2D fitted thermal conductivity λ and electrical conductivity σ of dry air plasma at atmospheric pressure as a function of temperature T.

where: T is temperature in [K], σ is electrical conductivity in [S/m], $\beta_1 = 150.2$, $\beta_2 = -9.59\text{x}10^5$ and $r^2 = 0.9981$. The TC2D fit of equation (3a), shown in Figure 2b, is based on 8 points at 7000K ≤ T ≤ 22000K.

However, for T < 10000K there are only two points which explains why the upward bend of the experimental curve σ(T) near σ=0 (Figure 2b) is not described by equation (3a) (see Figure 3b). An alternative fit that is suitable for this temperature interval (4000K ≤ T ≤ 8000K) is

$$\ln \sigma\,(T) = \gamma_0 + \gamma_1 T \qquad (3b)$$

where: $\gamma_0 = -1.3028$, $\gamma_1 = 0.001006$ and $r^2 = 0.9995$ (Figure 3c). Using the TC2D software [15], relations of the equations (3a), (3b) are shown graphically in Figures 3b, 3c.

3. Conversion of λ(T), σ(T), q(T) *to Functions of Heat Flux Potential* S(T)

Analytical form of equations provides an insight into the interrelationships of various properties. Thus, there are analysis advantages in converting λ (T), σ(T), q(T) as functions of temperature into functions of heat flux potential S(T) which is given by [1, 16]

$$S\,(T) = \int \lambda\,(T)\,dT \qquad (4)$$

where: S = 0 at $T\big|_{\sigma=0}$ = 7000K.

Using equations (1) and (4) we have,

$$S\,(T) = \sum_{i=0}^{N} \alpha_i\, T^{i+1}/(i+1) \qquad (5)$$

where: N=7. An expression with 4 parameters provides a fit for the inverted dependence T = T (S),

$$T\,(S)\,/1000 = a + bS^3 + c(\ln S) + d/S^{1.5} \qquad (6)$$

where: T in [K], S in [kW/m], a=1.7005, $b=6.741\text{x}10^{-5}$, c=4.551, d=7.232 and r^2=0.9993. Using the TC2D software, the calculated output of the equation (6) is shown in Figure 4 as Temperature T(S) versus Heat Flux Potential (S).

A reasonable fit in evaluating λ (T) for the low-temperature interval, 4000K ≤ T ≤ 10000K, with 4 parameters is,

$$1/\lambda = a + b(T/1000) + c(T/1000)^2 + d(T/1000)^3 \qquad (6a)$$

with a = 32.9, b = -12.5, c = 1.56, d = -0.0635; T in [K], λ in [W/(m K)]. Equation (6a) is supposed to be used instead of equation (1) in calculations for air plasma at 4000K ≤ T ≤ 10000K.

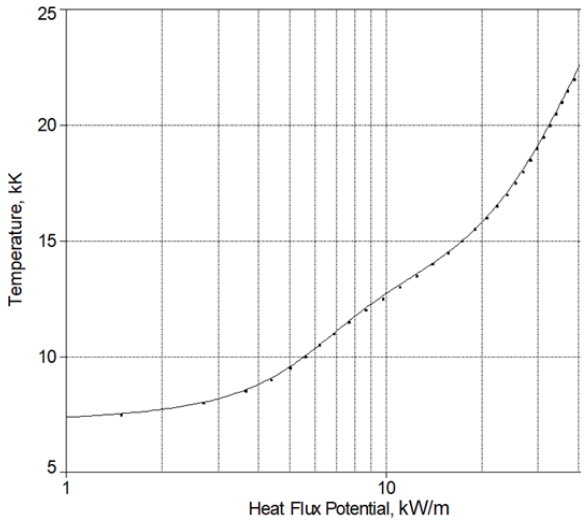

Fig. 4. TC2D fit for temperature T(S) as a function of Heat Flux Potential (S).

3a) Conversion of σ(T) *into* σ(S)

The conversion of electrical conductivity σ(T) into σ(S), as a function of heat flux potential, is achieved by substitution of equation (6) into equation (3a) to yield a polynomial of 7th order,

$$\sigma\,(S) = \sum_{i=0}^{N} \delta_i\, S^i \qquad (7)$$

where: N = 7, heat flux potential S is in [W/m], electrical conductivity σ is in [S/m], air plasma at atmospheric pressure is at 7000K < T ≤ 22000K and polynomial coefficients are δ_0 = 80.198764, δ_1 = -0.19363455, δ_2 = 2.6289597x10^{-4}, δ_3 = -3.3632063x10^{-8}, δ_4 = 2.0131845x10^{-12}, δ_5 = -6.3642008x10^{-17}, δ_6 = 1.0281437x10^{-21}, δ_7 = -6.6975965x10^{-27}, and r^2 = 0.99947688.

Our model needs values for the transport properties averaged over the interval 0 < S < S_0. It is stipulated that S = 0 at T = 7000K that is corresponding to σ = 0 (as shown in Figure 3b) and S = S_0 at the maximum temperature (assumed in the particular case study e.g., 20000K). The mean conductivity σ_m is found by integrating σ(S)/S_0 over the interval {0, S_0}, to give $\sigma_m(S_0)$ approximated by a polynomial of 6th order (TC2D)

$$\sigma_m(S_o) = \sum_{i=0}^{N} \gamma_i\, S^i \qquad (8)$$

where: N = 6, heat flux potential S and S_0 is in [W/m], mean conductivity σ_m is in [S/m], dry air plasma at atmospheric pressure and 7000K < T ≤ 22000K, polynomial coefficient are γ_0 = 181.1, γ_1 = -0.0560, γ_2 = 6.80x10^{-5}, γ_3 = -5.59x10^{-9}, γ_4 = 2.11x10^{-13}, γ_5 = -3.85x10^{-18}, γ_6 = 2.74x10^{-23} and r^2 = 0.99994.

The variation of mean conductivity $\sigma_m(S_0)$ with Heat Flux Potential (S_0) is shown in Figure 5.

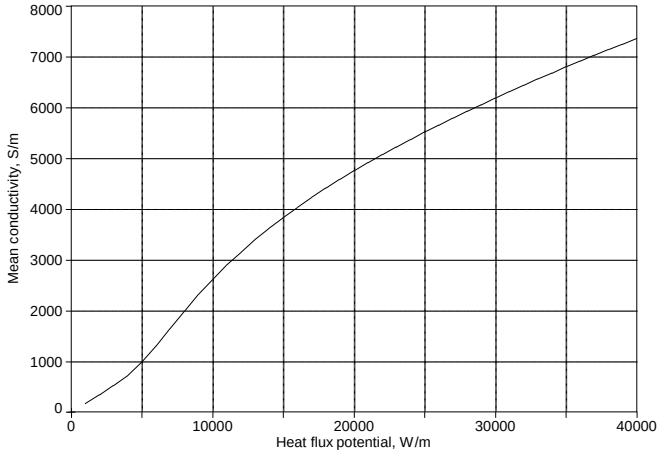

Fig. 5. Graph of mean (0 < S ≤ S_0) conductivity σ_m computed by TC2D as a function of heat flux potential S_0.

3b) Conversion of q(T) *into* q(S)

Using the full range of ε vs T data, Table I, TC2D offers a fit for the power flux density,

$$q\,(S) = a + b \sin\,(2\pi S/d + c) \qquad (9)$$

where: heat flux potential S is in [W/m], power flux density q is in [W/m^2] and coefficients of a ≈ b = 5.60 x 10^7, c = 4.33, d = 53.5, r^2 = 0.9998.

The equation (9) can be readily integrated in elementary functions

$$q_m\,(S_0) = a + F \sin\,(\pi S_0/d + c) \sin\,(\pi S_0/d) \qquad (10)$$

where: F is a formfactor (depends on the model).

The power flux density (power loss by optical radiation via unit surface of the emitting plasma), q(S) is represented by equation (9) along with other equations (Section III) and are used to evaluate the arc power losses. The arc power losses as a function of heat flux potential are shown in Figure 6.

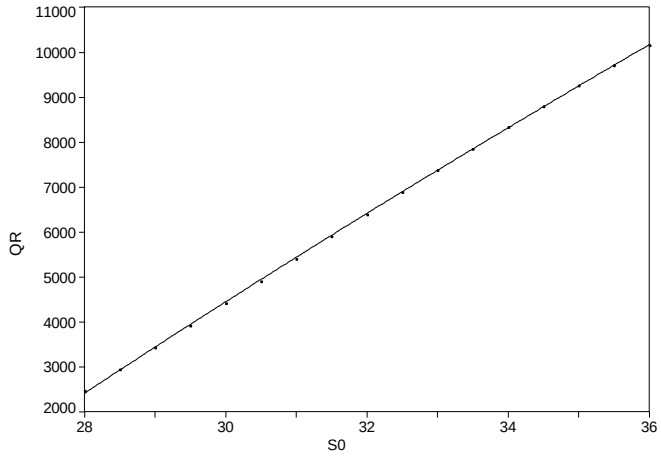

Fig. 6. Graph and TC2D fit for power of optical radiation Q_R [MW/m^3] as a function of heat flux potential S_0 in [kW/m], where: 28 ≤ S_0 ≤ 36 kW/m, see equation (25).

III. Formulation: Theoretical Basis, Equations and Solutions

A. Basic Arc Column Model (Elenbaas-Heller Arc Theory)

In the proposed arc column model the main assumptions for the Elenbaas-Heller's theoretical description of the arc column has been introduced:

- Thermal equilibrium plasma.
- Cylindrical symmetry, electric potential gradient acting along the plasma column axis, all parameters independent of the axial coordinate as the arc radius is the same along the column as measured on photographs, constant pressure (atmospheric).
- Steady state conditions.
- Magnetic field and gas flow effects are not considered at this stage as we do not include momentum balance where magnetic and gas flow effects are important.

The basic model of the arc column introduced in Elenbaas-Heller equations is based upon the following equations,

$$\sigma (S)\, E^2 = - (1/r)\, d/dr\, (r\, dS/dr) + Q_R \qquad (11)$$

where: $S(0) = S_0$, $dS/dr\,(0) = 0$

$$I = 2\pi\, E \int_0^{r_0} \sigma (S)\, r\, dr \qquad (12)$$

where: r is the radial coordinate in [m], I is the arc current in [A], r_0 [m] is the arc radius at $T = T_{r0}$, $T_{r0} \geq T_a$ (ambient temperature), σ is the electrical conductivity in [S/m], E is the electric field [V/m], S is the heat flux potential in [W/m], Q_R is the power dissipated from the arc by optical radiation in [W/m^3].

B. Maecker's Model

The Maecker version of the Elenbaas-Heller's theoretical description of the arc column [1] has been used to formulate the model mathematically in finding the radial temperature distribution T(r), electric field E, radius r_0 of the electrically conductive zone ($\sigma > 0$). In this model for the radius $r > r_0$, $\sigma = 0$ at $T_{r0} \geq T \geq T_a$, with the ambient temperature $T_a << T_{r0}$. The Maecker theory for model was developed on the basis of Elenbaas-Heller-Steenbeck-Maecker theory for a wall-stabilized arc in a cylindrical channel [1]. The Maecker version proposed here is used for a free-burning arc.

C. Zarudi's Approximation

Equations (11) and (12) may be solved after assumption that the arc central core (maximum) temperature is $T(0) = T_0$ (and in particular for $T_0 = 2x10^4$ K) and the average electrical conductivity σ is constant, $\sigma = \sigma_m$, between T = 7000K and $T=T_0$, and zero for $T \leq 7000$K. The average (mean) electrical conductivity σ_m was calculated in this contribution. Thus, we obtain $\sigma_m \approx 7000$S/m calculated manually (integral of σ(S)/S evaluated by the method of rectangles [15]), $\sigma_m \approx 6500$S/m by equation (10).

Equations (11) and (12), may be written with as [1]

$$\sigma_m E^2 = Q_C + Q_R = -(1/r)\, d/dr\, (r\, dS/dr) + Q_R \qquad (11a)$$

$$I = \pi\, r_0^2\, \sigma_m\, E \qquad (12a)$$

where Q_C is the conduction of heat power losses. The electric field of the arc core without and with the power losses is estimated via the arc radiation (Q_R).

D. Solution Without Optical Power Losses Via the Arc Radiation, $Q_R = 0$

In the absence of optical radiation losses ($Q_R = 0$ in equation (11a)), the electric field E is designated by Φ (i.e. $\Phi = E|_{Q_R=0}$). This leads to equations (11), (12) taking the form

$$\Phi\, r_0 = 2[(S_0 - S_{r0}) / \sigma_m]^{1/2} \qquad (13)$$

$$I = \pi\, r_0^2\, \sigma_m\, \Phi \qquad (14)$$

where: r_0 is the arc radius. It is convenient to set $S_{r0} = 0$.
At $T = 2x10^4$ K according to equation (6) and Figure 4 $S_0 = 3.24 \times 10^4$ W/m. With σ_m from Figure 5 the dependence of the equation (13) in a graphical form is shown in Figure 7.

The solution for Φ is,

$$\Phi = 4\pi\, S_0 / I \qquad (15)$$

which for I = 1.25 kA calculates, Φ = 326 V/m

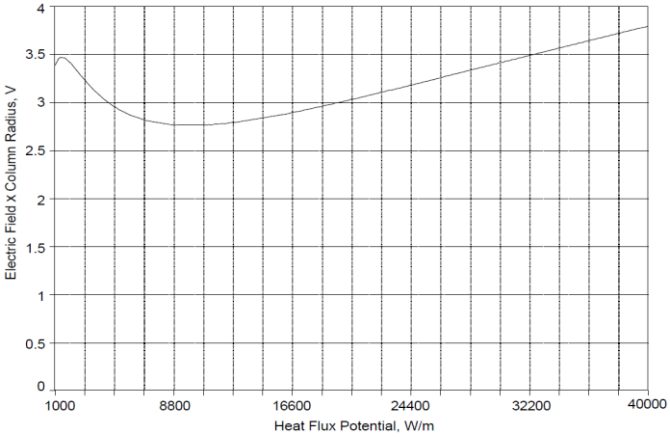

Fig. 7. Similarity parameter $\Phi\, r_0$ versus Heat Flux Potential (TC2D).

Equations (13) and (15), if the latter is written as

$$\Phi\, I = 4\pi\, S_0 \qquad (15a)$$

can be interpreted as follows:

- In equation (15a), power of Ohmic heating per unit length of arc column produces relevant rise of heat potential with 4π being a geometrical formfactor.

- In equation (13), the similarity parameter Φ r_0 [V] does not explicitly depend on the arc current I, via S_0 and σ_m it depends on the axial temperature T_0.

For evaluation of Φ at different arc currents Figure 4 can be used, if the abscissa axis is re-scaled to 4π S_0 / I. Similarly, a diagram for estimating similarity parameter Φ r_0 is prepared, Figure 7.

As the power losses via the arc optical radiation losses are ignored ($Q_R = 0$), the equation (11a) reduced to

$$\sigma_m \Phi^2 = -(1/r)\, d/dr\, (r\, dS/dr) \qquad (16)$$

and can readily be solved with the boundary condition $S(0) = S_0$, $dS/dr\,(0) = 0$ in the form

$$S = S_0 [1 - (r/r_0)^2] \qquad (17)$$

The relation (equation (17)) is sometimes (e.g. [2]) referred to as "the parabolic solution". Such radial profile of S is valid for any plasma-forming gas if the optical radiation is ignored and constant conductivity $\sigma = \sigma_m$ is stipulated.

For air, in the present case, the equation (17) may be combined with Figure 4 to yield the temperature as a function of the radial coordinate as shown for several values of the axial temperature in Figure 8.

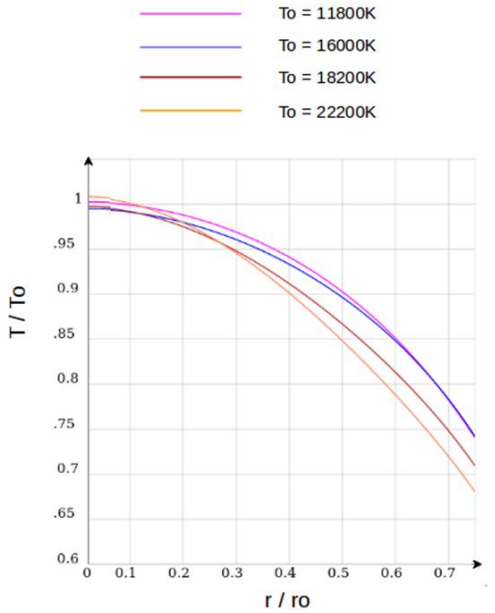

Fig. 8. Radial profiles of the temperature computed by using TC2D [15] for different temperatures at r = 0 with no optical radiation losses with Maecker-Zarudi model [1], (The curves have been artificially slightly shifted vertically to avoid superposition near r = 0).

E. Solution With Optical Power Losses Via the Arc Radiation, $Q_R \neq 0$

The power flux density (power loss by optical radiation via unit surface of the emitting plasma, q(S), was presented by equation (9).

Zarudi's model [1] requires averaging of q(S) in the interval of $0 \le S \le S_0$. Before studying the case of combined power losses, by conduction of heat and radiation, we consider the case of pure radiative losses (zero conductive loss) that is feasible at extremely high arc currents. Note that at higher arc currents radiation power losses dominate. If conductive losses are ignored, instead of equation (15a) Maecker-Zarudi model predicts as follows,

$$\mathcal{E}\, I/r_0 = 2\pi\, q_m \qquad (18)$$

where: $\mathcal{E}$ is the electric field in the extreme case of a plasma column with power losses by radiation alone; $q_m = r_0 Q_R/2$ is a function of S_0 which depends on the way q is averaged to obtain q_m.

Let $\mathcal{E}$ be the value of electric field E which is (for the moment) calculated from

$$\mathcal{E}\, I = Q_R\, \pi r_0^2 = Q \qquad (19)$$

where [1] we define:

$$Q_R = 2/r_0 \int_0^{S_0} q(S)\, dS/S_0 \qquad (20)$$

Comparing with the equation (10) the formfactor is $F = bd/(2\pi S_0)$. For I ~ 1000A and $\mathcal{E}$ ~ 10 V/cm, as it is in our case study of the rotary arc, we estimate for r_0 = 0.7cm (using optically visible 1.25kA quasi-dc arc plasma column radius, measured on photographs [6, 7]) from the equations (10) and (19)

$\mathcal{E}\, I \sim 1\text{x}10^4$ W/cm, $Q \approx 1.68\text{x}10^4$ W/cm, so that for $Q_R > \mathcal{E}\, I$

As according to the energy conservation law, always $Q \le \mathcal{E}\, I$, there is something wrong with this (optical) part of Zarudi's model [1]. Here we propose an alternative form of equation (10) with different formfactor F. The total emission is a sum of emission from ring-shaped portions each being proportional to the area $2\pi r\, dr$ (where, dr is ring's width). The integral in equation (20) underestimates the contribution to radiation from peripheral parts of the arc column where r is larger. Each portion emits,

$$dQ = q(r)\, (dr/l) 2\pi r \qquad (21)$$

where: q(r) = q(S(r)), S(r) are from the equation (17), and l = 1 cm is the reference thickness of the radiating layer as it is taken from Avilova *et al* [13]. After combining equations (9), (17), (21) and integration we obtain relationship of the form,

$$q_m(S_0) = r_0 Q_R/2 = \pi r_0^2/l\, (a + (bd/\pi S_0) \sin(\pi S_0/d + c) \sin(\pi S_0/d)) \qquad (22)$$

and now evaluate $Q/(\mathcal{E}\, I) \approx 0.67 < 1$. Thus, it is seen that such modification of Zarudi's model can be used to treat the case of combined power dissipation $Q_C + Q_R$ as follows.

To determine the real electric field the quadratic equation obtained from equations (11a) and (12a) not neglecting Q_R may be solved,

$$E = \Phi (\sigma_m E^2) / (\sigma_m E^2 - Q_R) \quad (23)$$

and use the solution that is > 0,

$$E = \Phi/2 + [(\Phi/2)^2 + Q_R/\sigma_m]^{1/2} \quad (24)$$

To evaluate Q_R [MW/m^3] the simple approximation presented by Figure 6, was used with A = -55470, B = 10938.

$$Q_R = A + BS_0^{0.5}, \quad (25)$$

The relationship (equation (25)) is suitable for the range $28 \leq S_0 \leq 36$ kW/m. For $0 \leq S_0 \leq 36$ kW/m, equation (22) is suitable with $a \approx b = 5.60 \times 10^7$, c = 4.33, d = 53.5.

For the arc current of I = 1.25kA and maximum arc core axis temperature of $T_0 = 2x10^4$ K, this model (integrals evaluated by the method of rectangles [14]) yield an electric field of E = 1106V/m and, from $r_0^2 = I/(\pi\sigma E)$ electrically conductive zone radius of $r_0 = 0.74$cm. The same calculation performed by TC2D [15] yields E = 1190V/m and $r_0 = 0.72$cm.

IV. Validation of the Modified Zarudi Model

A. Comparison with Exact Numerical Calculations

With our best fits for the dependencies S = S(T) and σ = σ (S) introduced in the equations (5) and (7), it is possible to numerically solve Elenbaas- Heller equation without radiation power losses, and the solution may serve as a reference example for the radial profile of the temperature for the particular value of the temperature on the arc column axis e.g., $T_0 = 2x10^4$ K. The starting equation (11a),

$$\sigma (S) E^2 = - (1/r) d/dr (r dS/dr) + Q_R \quad (11a)$$

with $Q_R = 0$, boundary conditions $S(0) = S_0$, $dS/dr(0)=0$ and dimensionless variables

$$x = r/r_0 , y = S/S_0 \quad (26)$$

takes the form

$$y'' + (1/x)y' + f(y) = 0$$
$$y(0) = 1, y'(0) = 0 \quad (27)$$

$$f(y) = \sum_{k=0}^{N} b_k y^k \quad (28)$$

In principle, equations (27, 28) are valid and can be used not only within the numerical approach to the problem, but also when approximate models are used, as seen from Table II.

TABLE II
PARAMETERS IN THE FUNCTION f(y)*

Case studies:	N	b_0	b_1	b_k, k > 1
1) Numerical solution of Elenbaas-Heller equation	7	≠ 0	≠ 0	≠ 0
2) Our model (Zarudi's model)	1	≠ 0	0	0
3) Maecker's linearisation model	1	0	≠ 0	0

*where: N, b_0, b_1, k are parameters in the function f(y) of the equation (28).

The exact calculations were conducted using an on-line differential equation solver [17]. This is an educational software with no indication of a converged solution. However, the user can specify the number of computational steps, default value of 100. With 200 steps the graphical output is the same, confirming a converged solution. An example of calculation results for S_0 = 32400 W/m, (i.e. maximum arc core axis temperature of $T_0 = 2x10^4$ K) is shown in Figure 9.

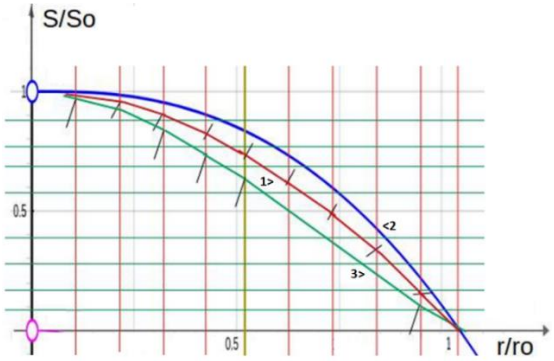

Fig. 9. Heat flux potential as a function of radial coordinate calculated without the radiation loss by various models: the model of the present paper (parabolic - brown line (1)), by solving equation (11) numerically (blue line (2)) and by Maecker's linearised model (Bessel - green line (3)) [1].

Figure 9 shows that the proposed modified Zarudi model without radiation loss provides computational results for the radial temperature profile that are closer to the exact numerical results than those obtained by Maecker's linearisation model. This can be explained by the S-shaped σ (T) dependence for air plasma, not so well pronounced for inert gases [1].

B. Comparison with Experimental Measurements

The modified Zarudi theoretical model correctly predicts the voltage gradient (electric field intensity E) and the radius of electrically conductive core r_0 of the arc plasma column. Experiments with free burning arcs provide mostly data on the arc electric parameters – current I and arc burning voltage U (electric potential difference) measured across the arc electrodes, and radius of the luminous plasma column r_1 that is evaluated from photographs of the arc.

From the model, total arcing voltage is estimated as a sum of the cathode fall (~20V) and the product of calculated electric field E and arc length. Note that based on the previous research work [18-20], cathode fall voltage for high-current arcs with

copper electrodes is assumed as 16V and 4V is also added for the transitional (constriction) zone.

There are reasons for the conducting radius r_1 not to be equal to the optical radius r_0. All image recording devices have a limited range of sensitivity so that the recorded "boundary" of the luminous plasma column in fact is where light intensity level is at the threshold of the imager. The emissivity of air [13] is rapidly reduced below 14000K which enhances the strong dependence (as T^4, see equation (1)) of optical output Q_R. Thus, if for the case study with maximum temperature of 20000K we assume that the visible column boundary, $r = r_1$, is at $T = 14000$K, the value of r_1 can be estimated as follows. By using the dependence of T on S (Figure 3), on the curve calculated for 20000K we read the value at $T = 14000$K which is $S = S_1 = 13.96$kW/m. With $S_1/S_0 = 0.431$, equation (17) is used to find r_1/r_0. For the case study with maximum temperature of 20000K the present model predicts $r_0 = 0.72$ cm so that,

$$r_1 = r_0 (1 - S_1/S_0)^{1/2} \approx 0.55 \text{ cm}$$

Although there is generally only a limited amount of experimental data currently available, for technically different arc discharges, the various potential arc models may be compared albeit to a limited extent.

TABLE III
COMPARISON OF EXPERIMENTAL AND THEORETICALLY CALCULATED PARAMETER VALUES (ARC VOLTAGE, U AND ARC CHANNEL RADIUS, r_1) FOR THREE DIFFERENT ARC TYPES (RAD, EAF, LRS)

Case /Test current	Position of arc channel	Contamination of air	Data	U [V]	r_1 [cm]	T_0 [kK]	Radiation
EAF, 600A	Vertical	By vapour of melted material	Theory	150	0.95*	16	No
			Experiment	190	0.90	---	---
LRS, 100A	Horizontal	No	Theory	480	0.80*	10	No
			Experiment	500	0.90	---	---
RAD, 1.25kA	Vertical	No	Theory	130	0.55	20	Yes
			Experiment	140	0.40	---	---
	Vertical and Horizontal	By degraded PTFE	Theory	490	---	20	Yes
			Experiment	430	---	---	---

where: "EAF" is the Electric Arc Furnaces [10]; "LRS" is the Lightning Return Strike [21]; "RAD" is the B-Field Rotary arc device [6] (Figure 1c); "U[V]" is the arc voltage; "r_1" is the visible arc column radius; "T_0" is the arc temperature; "Radiation" is the arc model included radiation losses. Note, *$r_1 = r_0$, the quasi-dc arc column lengths are measured on photographs.

Results for three different groups of free burning arcs may be considered. These groups are electric arc furnaces (EAF) [9], lightning return strike (LRS) [21], [22] and electromagnetically controlled arcs such as those used in some DC circuit breakers: rotary arc devices (RAD) [6], [8], Table III compares results obtained with the various arc models for these three types of free burning arcs. Column 1 (Case/Test current) indicates which of the three types of free burning arcs are evaluated. Column 2 (Position of arc channel) indicates if the arc was vertical or horizontal. Column 3 (Contamination of air) indicates the presence of contamination (where the PTFE is Polytetrafluoroethylene). Column 4 (Data) indicates if the data was experimental or theoretical. Column 5 (U [V]) lists the arc voltages. Column 6 (r_1 [cm]) indicates the visible arc column radius. Column 7 (T_0 [kK]) indicates the temperature of the luminous arc core. Column 8 (Radiation) indicates if optical radiation loss was included.

For the arc furnace case (EAF), the model with no radiation losses and experimental values of arc voltage were similar (150V, 190V) as were the arc radii (0.95cm, 0.90cm). The arc model predicted an arc temperature of 16000K, but no experimental value was available. For the lightning return case (LRS), the arc model with no radiation losses and experimental values of arc voltage were similar (480V - model compared with 500V - experimental). The arc radius theoretically was 0.80cm compared with 0.90cm experimentally.

Data are available for electromagnetically controlled electric arcs (RAD) which enable a comparison to be made of theoretical model predictions with the inclusion of optical radiation losses (Table III). For the rotary arc group (RAD), vertical (arc length of 93mm) and vertical & horizontal (arc length of 397mm), the model results show good agreement for the arc voltage with test results obtained with arcs ignited by exploded wire (130V with 140V vertical arc; 490V with 430V vertical & horizontal arc) [6-7]. For the vertical arc the model radius (0.55cm) showed good agreement with experiment (0.40cm). The arc temperature (T) was identical for the experiment and the model value (20000K).

Results of laboratory simulation [21] of LRS [22] by a d.c. arc in open air are compared with the predictions of our model for current of 100A. Temperature of 10000K as calculated is compatible with measured values [22].

In summary, the modified Zarudi theoretical model is one-dimensional, without time dependence and without prescribing external boundary condition. This makes the model economical in terms of time consumption in calculating the electric arc parameters with reasonable accuracy. This may cause difficulties matching the proposed model with the computational algorithms that are used in specialized Computational Fluid Dynamics (CFD) software, for example ANSYS Fluent (CFD). Thus, publishing this contribution will bring this problem to readers' attention.

V. CONCLUSION

A mathematical model of free burning arcs including optical radiation losses has been presented. This model prescribes a reasonable value for the maximum temperature (e.g., 20000K) of the arc plasma. The calculations of electric field and column radius are in fair to good agreement with experimental data.

In summary, the conception of a cylindrical, current-carrying channel with constant (radially and axially) conductivity is found to be suitable to describe the arc plasma column in open air at moderate currents (10^2 to around 10^3A).

REFERENCES

[1] Dresvin S. V., (ed.), "Physics and technology of low-temperature plasma" (in Russian), Publisher: Atomizdat, Moscow, USSR, 1972. Publisher (English translation): Iowa State University, 1977.

[2] Pflanz, H. M. J., "Steady State and Transient Properties of Electric Arcs", dissertation, Technische Hogeschool Eindhoven, 1967. [Online]. Available: https://doi.org/10.6100/IR144184

[3] Boulos M. I., Fauchais P., Pfender E., "Thermal plasmas fundamentals and applications" Publisher: Plenum Press, New York, 1994.

[4] Raizer Y. P., "Gas discharge physics", Publisher: Springer Verlag, Berlin, 1991.

[5] Finkelnburg W., Maecker H.,"Elektrische Bőgen und thermisches Plasma", "Gasentladungen II" (S Flűgge, ed.), Handbuch der Physik, vol. 22. Publisher: Springer Verlag, Berlin, 1957.

[6] Shpanin, L. M., Jones, G. R., Spencer, J.W, "The production of plasma pulses with convoluted arc columns in atmospheric pressure air", IEEE Transactions on Plasma Science, Vol. 38, No. 3, pp.509-515, March 2010.

[7] Shpanin, L. M., "Electromagnetic arc control for current interruption", Ph.D. thesis, University of Liverpool, Liverpool, U.K., 2006.

[8] Shpanin, L.M., Kidman, M. C., Humphries, J. E., Spencer, J. W., Jones, G. R., "The interaction of high current electric arcs with spatially varying cross magnetic fields", Proceeding of the 15th Int. Conf. on Gas Discharges and their Applications, Toulouse, France, pp.183-187, 2004.

[9] Bowman B., Jordan G. R., Fitzgarald F., "Physics of high-current arcs", June 1969 (uploaded 2018). [Online]. Available: https://www.researchgate.net/publication/293511993_PHYSICS_OF_HIGH-CURRENT_ARCS

[10] Pauna H., Aula M., Echterhof T., Huttula M., Fabritius T., "Electric arc voltage-length and conductivity characteristics in a pilot-scale AC electric arc furnace", Metallurgical and materials transactions B, Vol. 51, pp. 1646–1655, June 2020.

[11] Cressault, Y., "Basic knowledge on radiative and transport properties to begin in thermal plasmas modeling", AIP Advances, 5 057112, pp.1-17, May 2015. [Online]. Available: https://aip.scitation.org/doi/10.1063/1.4920939

[12] Wang C., Wu Y., Chen Z., Yang F., Feng Y., Rong M., Zhang H., "Thermodynamic and transport properties of real air plasma in wide range of temperature and pressure", *Plasma Science and Technology*, Vol.18, No.7, pp.732-739, Jul. 2016.

[13] Avilova I. V., Biberman L.M., Vorobiev V. S., Zamalin V. M., Kobzev G. A., Lagarkov A. H., Mnatsakanyan A. X., Norman G. Uh., "Optical properties of hot air", Publishing house Science, Moscow, USSR,1970.

[14] Courses in Mathematics and Statistics at the University of West London, Chapter 7, 2023. [Online]. Available: https://www.ucl.ac.uk/~zcahge7/files/week9.pdf

[15] TableCurve 2D: Automated Curve Fitting and Equation Discovery: Version 5.01 for Windows; User's Manual, Publisher: SYSTAT 2002, ISBN 818834107X, 9788188341078.

[16] Fridman, A., Kennedy, L. A., "Plasma Physics and Engineering", CRC Press, 2011.

[17] Calculator for 2x2 differential equation systems1.order, 2023. [Online]. Available: https://elsenaju.eu/Calculator/ODE-System-2x2.htm (Copyright the Closure Library Authors).

[18] Dickson, D. J., Engel, A. von, "Resolving the electrode fall spaces of electric arcs", Proceedings of the Royal Society of London. Series A, Mathematical and Physical Sciences, Published by Royal Society, Vol. 300, No. 1462, pp. 316-325, Sep. 1967.

[19] Kesaev I. G., "Cathode Processes in Electric Arcs" Publisher: Nauka, Moscow, 1968.

[20] Keidar M., Beilis I. I., "Plasma engineering (second edition"). Publisher: AP Elsevier, Cambridge, Massachusetts, 2018.

[21] Stokes A. D., Oppenlander W. T., "Electric arcs in open air", J.Phys.D:Appl.Phys., Vol.24, pp.26-35, 1991.

[22] Sousa Martins R., Zaepffel C., Chemartin L., Lalande P., Lago F., "Characterization of high current pulsed arcs ranging from 100 kA to 250 kA peak" J.Phys.D:Appl.Phys., 2019 [Online]. Available: https://www.researchgate.net/publication/330609580

Boyan E. Djakov received the M.Sc. Degree in physics from Moscow State University, Russia, the Ph.D. degree in physics from the University of Liverpool, U.K., and the D.Sc. degree from Bulgarian Academy of Science, Sofia, Bulgaria. He was a Head of the Laboratory of Plasma Physics and Engineering, Institute of Electronics - Bulgarian Academy of Science, an Adjunct Professor of natural science at the American University in Bulgaria, Blagoevgrad, and an Adjunct Professor in plasma physics at Sofia University "Saint Kliment Ohridsky", Sofia, Bulgaria. For two terms of office, he was a member of the Executive Council of the Bulgarian Academy of Sciences. Currently, he is a consultant with the NUCLEUS Plasma Test Laboratory, Sofia, Bulgaria.

Leonid M. Shpanin (Senior Member, IEEE) received the M.Sc. degree in radio engineering from Azerbaijan Technical University, Baku, Azerbaijan, and the Ph.D. degree in electrical engineering from the University of Liverpool, Liverpool, U.K. He is a Senior Lecturer in Electronic Engineering, Department of Engineering and Mathematics, Sheffield Hallam University, Sheffield, U.K. Dr. Shpanin is a guest member of an international study Low-Voltage group on switchgear arcs, which is a part of the Current Zero Club and a fellow of the higher education academy, UK.

Gordon R. Jones received the B.Sc. degree in physics from the University of Wales, Cardiff, U.K., the Ph.D. degree in physics from the University of Liverpool, Liverpool, U.K., and the D.Sc. degree from the University of Wales. He is currently an Emeritus Professor and an Honorary Senior Research Fellow with the University of Liverpool, where he was the Head of the Department of Electrical Engineering and Electronics, Head of the Arc Research Group, and Director of the Centre for Intelligent and Monitoring Systems. He is the author of several books in the area of chromatic monitoring, high-pressure arcs, and SF6 switchgear. Prof. Jones is a member of the Executive Management Committee of the International Series of Conferences on Gas Discharge and Their Applications and of an international study group on switchgear arcs, which is the Current Zero Club. He was the recipient of the Institution of Electrical Engineering (IET) Science, Education and Technology Achievement Medal in 1999 and of a Medal of Distinction by the Academy of Sciences, Bulgaria, in 2006. He was a fellow of the IET, U.K., and a member of the Institute of Physics, U.K.

Joseph W. Spencer received the B.Eng. and Ph.D. degrees in electrical engineering from the University of Liverpool, Liverpool, U.K. He is a Professor of electrical engineering, with the University of Liverpool, where he was the Head of the Department of Electrical Engineering and Electronics, Head of the School of Electrical Engineering, Electronics and Computer Science. He is currently the Director of the Centre for Intelligent and Monitoring Systems, University of Liverpool. Prof. Spencer is a member of an international study group on switchgear arcs and the Honorary Treasurer of the International Series of Conferences on Gas Discharge and Their Applications. He is a member of the Institution of Electrical Engineering, U.K.

Jiu Dun (Joseph) Yan (Senior Member, IEEE) graduated from Tsinghua University (Beijing) with BEng in 1986 and MEng in 1988 in engineering mechanics and obtained the PhD degree in electrical engineering from the University of Liverpool in 1998. He is currently Professor of Applied Electro-magnetism at the University of Liverpool, with research interests in theory of SF_6 alternative gases for switching applications, simulation and experiment of switching arcs, novel switching and insulation technology, and energy storage systems. Professor Yan sits on the scientific committee of two international conferences (Physics of Switching Arcs and Gas Discharges and Their Applications). He is also a member of the Current Zero Club.